

Full-Space and High-Scanning Rate Leaky-Wave Antenna Based on Spoof Surface Plasmon Polaritons

Zhicheng Wu , Jun Wang , *Member, IEEE*, Lei Zhao , *Senior Member, IEEE*,
and Zhongxiang Shen , *Fellow, IEEE*

Abstract—A full-space and high-scanning-rate leaky-wave antenna (LWA) based on spoof surface plasmon polaritons (SSPPs) is proposed, which consists of the SSPPs design and rectangular periodic metal patches. Electromagnetic (EM) waves are transmitted along the SSPPs and coupled to the metal patches to generate fast radiation waves, which can achieve back-to-front frequency beam scanning performance. Additionally, the radiation mechanisms of the design are explained by the dispersion relationship, space harmonics and electric field distributions. The proposed LWA radiates energy based on -1 order space harmonic, which can realize full space and high beam scanning rate performance by controlling the period of the patches. Simulation results show that the LWA realizes a full space beam scanning from -90° to 90° within the 12.9 to 16.5 GHz frequency band, while the antenna also maintains a high scan rate of 7.35%/°.

Index Terms—High-scanning rate, spoof surface plasmon polaritons, leaky-wave antenna (LWA).

I. INTRODUCTION

LEAKY-WAVE antenna (LWA) is an antenna with unique radiation characteristics, which is extensively applied to wireless devices due to its high directionality, high gain and frequency scanning characteristics. Most of the LWAs are based on traditional structures, such as substrate integrated waveguide (SIW), microstrip line, and Goubau line [1], [2], [3]. However, the scanning angle and scanning rate of most of these LWAs are not wide and high enough. Recently, LWAs based on SSPPs have been proposed to provide new ideas to solve the above problems, which can realize wide-angle beam scanning and high-scanning rates.

Manuscript received 20 September 2023; revised 31 October 2023; accepted 10 November 2023. Date of publication 16 November 2023; date of current version 5 February 2024. This work was supported in part by the National Science Foundation of China under Grant 62201575; in part by the Science and Technology on Antenna and Microwave Laboratory Foundation under Grant 6142402220310; and in part by the Open Project of State Key Laboratory of Millimeter Waves under Grant K202310. (*Corresponding author: Lei Zhao.*)

Zhicheng Wu and Lei Zhao are with the School of Information and Control Engineering, China University of Mining and Technology, Xuzhou 221116, China (e-mail: zcwumax@cumt.edu.cn; leizhao@cumt.edu.cn).

Jun Wang is with the School of Information and Control Engineering, China University of Mining and Technology, Xuzhou 221116, China, also with the Science and Technology on Antenna and Microwave Laboratory, Xidian University, Xi'an 710071, China, and also with the State Key Laboratory of Millimeter Waves, School of Information Science and Engineering, Southeast University, Nanjing 211189, China (e-mail: jun-wang@cumt.edu.cn).

Zhongxiang Shen is with the School of Electrical and Electronic Engineering, Nanyang Technological University, Singapore 639798 (e-mail: ezxshen@ntu.edu.sg).

Digital Object Identifier 10.1109/LAWP.2023.3333259

Spoof surface plasmon polaritons (SSPPs) are a special EM mode in terahertz and microwave bands. Recently, many microwave devices based on SSPPs were proposed [4], [5], [6], [7], [8], [9], [10], [11], [12], [13], [14], [15], [16], [17], [18], [19], [20], [21], [22], [23], [24], [25], [26], such as filters [5], [6], [7], [8], [9], [10], [11] power dividers [12], circulators [13] and antennas [14], [15], [16], [17], [18], [19], [20]. Among SSPP-based antenna designs, the LWA can achieve wide beam-scanning angles and high scanning-rate characteristics. However, it is still difficult to design LWA which can realize full-space, high-scanning-rate and miniaturization performance.

According to the literatures, LWAs have been designed based on several SSPPs structures [21], [22], [23], [24], [25], [26], [27], [28], [29], [30]. In [21], an LWA based on circular metallic patches was proposed, which can achieve 55° beam scanning angle. However, its beam scanning angle needs to be improved. Thereupon, a wide-angle frequency-controlled beam scanning antenna based on the higher-order modes of SSPPs was proposed in [24], whose beam scanning angle covers from -66° to 63° within 11.7 to 50 GHz. Nevertheless, the wide operating bandwidth of this beam-scanning antenna is not conducive to designing the high beam scanning rate LWA. Accordingly, an LWA based on SIW-SSPPs with a high-scanning rate was proposed in [26], which covers the scanning angle of 123° . Therefore, designing an LWA with full-space scanning, high-scanning rate, and miniaturization performance is technically very challenging.

In this letter, a full-space and high-scanning-rate LWA based on SSPPs is proposed. The SSPP design is the feeding structure for the rectangular periodic metallic patches, which can transform the slow waves into fast waves to generate full-space and high-scanning-rate beam scanning waves by choosing the appropriate period of the patches. Additionally, the dispersion relationship, space harmonics and electric field distributions are analyzed in detail to explain the radiation mechanism. The proposed antenna has the following advantages:

- 1) The beam scanning range up to 180° .
- 2) The antenna has a high scanning rate of 7.35%/°.
- 3) The antenna has a compact size, which can be easily fabricated and has potential applications in radar and satellite systems.

II. THEORETICAL ANALYSIS AND ANTENNA DESIGN

A. SSPPs Feeding Structure

The configuration of the proposed SSPPs is shown in Fig. 1(a), which is printed on an F4B substrate of 0.5 mm thickness, dielectric constant of 2.65, and loss tangent of 0.0015. The

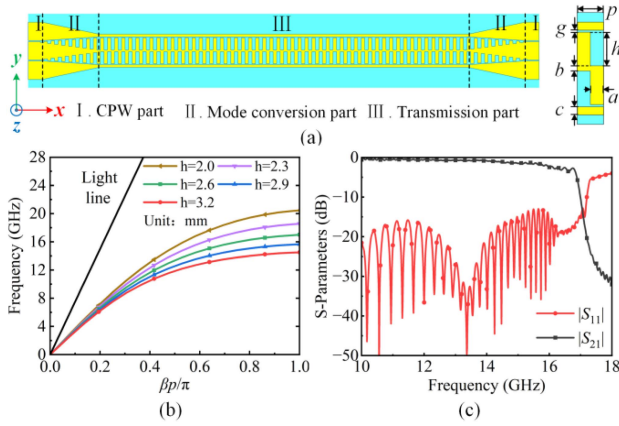


Fig. 1. (a) Configuration of the proposed SSPPs design and the SSPPs unit cell. (b) Dispersion curves of the proposed SSPPs unit cell with different h . (c) Simulated $|S_{11}|$ and $|S_{21}|$ of the proposed SSPPs.

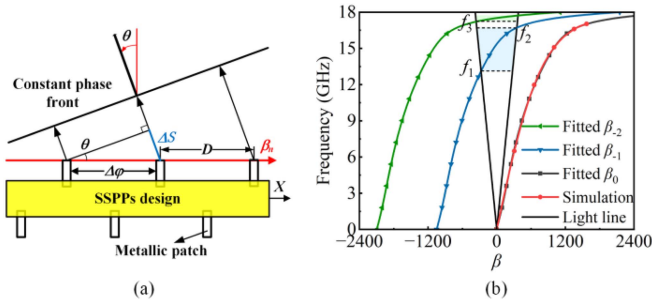


Fig. 2. (a) Radiation mechanisms model of the proposed LWA. (b) Simulated and fitted dispersion curves of different space harmonics modes.

SSPP structure consists of three parts: the coplanar waveguide (CPW), the mode conversion part, and the transmission section. The mode conversion part converts a quasi-TEM mode into TM mode, and the slow wave mode propagates in the transmission section. Fig. 1(b) shows the simulated dispersion curves of the SSPPs unit cell with different h , the geometrical parameters of the SSPPs unit cell are as follows: $a = 1$ mm, $b = 0.4$ mm, $c = 0.6$ mm, $g = 0.2$ mm, $p = 2$ mm, and $h = 2.6$ mm. From the simulated dispersion curves, we can clearly see that the dispersion relationship of SSPPs deviates from the light line, and the change of the propagation constant β becomes drastically even more when the frequency is adjacent to the asymptotic frequency, which indicates that the structure can support slow waves (SSPPs waves) propagating on its surface. Fig. 1(c) presents the transmission characteristics of the SSPPs design. It can be seen that the SSPPs design can achieve a high transmission efficiency when the frequency of the EM waves is below the cutoff frequency of 17 GHz, which is consistent with the simulated dispersion curves of the SSPPs unit cell given in Fig. 1(b).

B. Operating Principle of the Proposed LWA

A radiation mechanisms model of the proposed LWA is drawn in Fig. 2(a) to explain the operating principle. The radiation mechanism of the proposed LWA can be explained as follows.

- 1) The energy from the SSPPs is coupled to the bottom periodic metallic patches, which generates different phase

information between adjacent patches, and it can be expressed as (1).

- 2) The metallic patches radiate energy into free space. The EM waves on each patch have different path lengths to the wavefront, and cause the phase difference, which can be expressed by (2). According to (1) and (2), the direction of the beam can be predicted by (3).

$$\Delta\varphi_1 = \beta_n D \quad (1)$$

$$\Delta\varphi_2 = k_0 \Delta S \quad (2)$$

$$\theta = \arcsin(\beta_n/k_0) \quad (3)$$

where ΔS is the wave path difference between adjacent patches and $\Delta S = D \sin \theta$. β_n is the propagation constant of different order space harmonics caused by periodic perturbation

$$\beta_n = \beta_0 + \frac{2n\pi}{D}, \quad n = 0, \pm 1, \pm 2, \dots \quad (4)$$

where D is the period of perturbation, and β_0 is the fundamental mode propagating in the SSPPs. The phase difference between adjacent patches varies with frequency, which is the reason behind the frequency-control beam scanning characteristic of the proposed LWA [21].

According to the opening references and the space harmonic theorem, -1 order space harmonic is generally used to generate the beam scanning waves in the LWA. In our proposed design, a period parameter m is introduced to express the relationship between the period of the patch and the SSPPs unit cells ($D = mp$). According to (4), $n = -1$ space harmonic can be expressed as $\beta_{-1} = \beta_0 - 2\pi/m$. To exclude the interference of $n = -2$ space harmonic and even higher-order space harmonics on the performance of the LWA, a MATLAB fitting method is used to obtain a one-to-one correspondence functional relationship between β and f [31]. The fitting equation is as follows:

$$\beta_0(f) = a_1 \times e^{-\left(\frac{f-b_1}{c_1}\right)^2} + a_2 \times e^{-\left(\frac{f-b_2}{c_2}\right)^2} + a_3 \times d_1^{(f-d_2)} \quad (5)$$

where $a_1 = 4.351 \times 10^{18}$, $a_2 = 6.664 \times 10^4$, $a_3 = -152.2$, $b_1 = 57.93$, $b_2 = 80.92$, $c_1 = 6.707$, $c_2 = 32.12$, $d_1 = 0.7049$, $d_2 = -0.6561$. Based on (5), the fitting results and simulated dispersion relationship between β and f are presented in Fig. 2(b). It is clear to see that the fitted curve is very consistent with the simulated results. Meanwhile, the fitted curves of $\beta_{-1}(f)$ and $\beta_{-2}(f)$ can be calculated according to (4), which have three points f_1, f_2 , and f_3 of intersection with the light line. According to the Floquet theorem, f_1 and f_3 are the backfire frequency, f_2 is the endfire frequency. It should be noted that, in order to exclude the interference of -2 order space harmonic on the performance of the LWA, we need to adjust the value of m so that $f_3 > f_2$.

Combining (3) and (4), the relationship between m and f corresponding to f_2 and f_3 can be expressed as follows:

$$m_{f_2}(f) = 2\pi/[p(\beta_0(f) - k_0)]$$

$$m_{f_3}(f) = 4\pi/[p(\beta_0(f) + k_0)]. \quad (6)$$

Based on (6), the relationship between m and f corresponding to f_2 and f_3 is shown in Fig. 3(a). It is obvious to see that when $m < 5.27$, the condition $f_3 > f_2$ is satisfied. In order to ensure the lower limit of m , the relationship between m and scanning rate based on (4) and (5) is also shown in Fig. 3(a). It can be found that a smaller

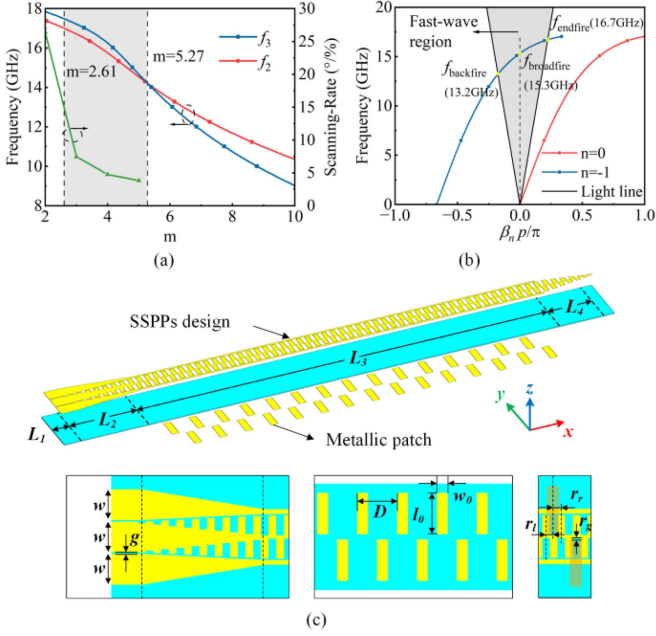


Fig. 3. (a) Relationship between m and f corresponding to f_2 and f_3 and the relationship between m and scanning rate. (b) Simulated dispersion relation of -1 order space harmonic and fundamental mode of SSPP unit cell. (c) Structure of the proposed LWA and the configuration of metallic patches.

value of m can achieve a higher beam scanning rate. Meanwhile, m should be greater than 2.61 due to the cutoff frequency of the proposed SSPPs is 17 GHz. Therefore, we select $m = 3$ for the LWA design to achieve high-scanning-rate performance. Fig. 3(b) shows the normalized dispersion relationship when $m = 3$. It can be clearly seen that part of the -1 order space harmonic is in the fast-wave region when the frequency ranges from 13.2 to 16.7 GHz. Meanwhile, the broad-fire frequency calculated from (5) is 15.3 GHz. In a word, the proposed LWA can theoretically achieve continuous back-to-front full-space beam scanning from 13.2 to 16.7 GHz and the scanning rate up to 7.46°/%.

C. Antenna Design and Simulated Results

Based on the previous theoretical and computational results, the LWA is proposed based on the SSPPs design in this section. Fig. 3(c) illustrates the structural distribution of the proposed LWA, which is printed on an F4B substrate of 0.5 mm thickness, dielectric constant of 2.65, and loss tangent of 0.0015. On the top layer of the substrate are the SSPPs, which have a single port and a tapering end. The tapering end is used to reduce reflection by radiating energy from the end of the transmission line into free space. On the bottom layer of the substrate is periodic metallic patches. In the previous discussion, it was concluded that the period D of the patches should be set to 6 mm, the distance between the bottom of the groove r_g and each patch is 0.2 mm, and the length and width of the rectangular patch are set to 6.2 and 1.6 mm, respectively. The detailed design parameters of the proposed LWA: $L_1 = 4$ mm, $L_2 = 16$ mm, $L_3 = 95$ mm, $L_4 = 12.5$ mm, $a = 1$ mm, $b = 0.4$ mm, $c = 0.6$ mm, $D = 6$ mm, $w = 4$ mm, $h = 2.6$ mm, $r_r = 0.6$ mm, $r_l = 0.4$ mm, $r_g = 0.2$ mm, $l_0 = 6.2$ mm, $w_0 = 1.6$ mm, $g = 0.2$ mm.

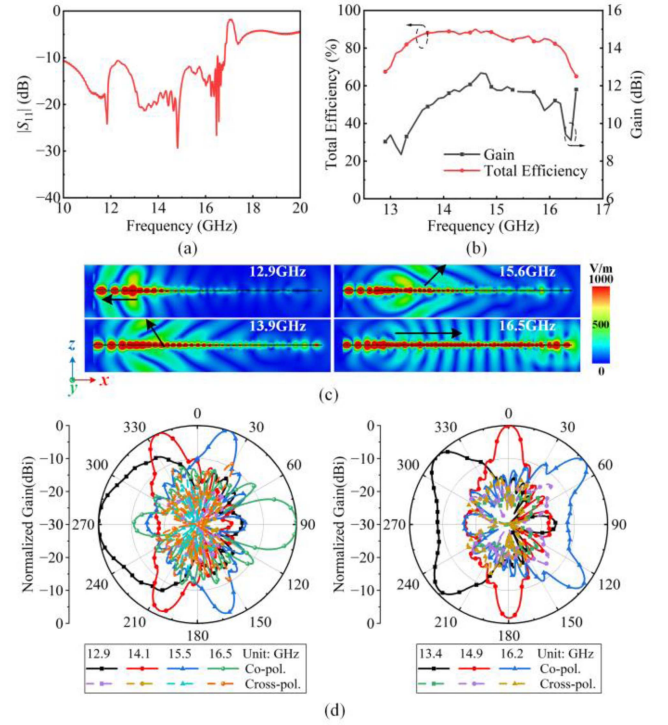


Fig. 4. Simulated results of the proposed LWA: (a) S -parameters; (b) peak gain and total efficiency; (c) electric field distributions at different frequencies on xoz -plane; (d) comparison between the copolarization and crosspolarization radiation patterns.

Fig. 4(a) plots the $|S_{11}|$, which was simulated by the commercial software CST; it can be clearly seen that the simulated reflection coefficient of the proposed LWA is less than -10 dB within the operating band of 12.9–16.5 GHz, it is in good agreement with the theoretical prediction. The simulated total efficiency and gain of the proposed LWA is presented in Fig. 4(b), which shows that the proposed LWA has a high efficiency and the average total efficiency is 83.6% over the operating band. Moreover, the average gain value of the proposed LWA is 11 dBi. Fig. 4(c) presents the simulated electric field of the proposed LWA in the xoz -plane at different frequencies. It is obvious that the angle of energy radiates out changes continuously with the change of frequency. It should be noted that the simulated end-fire radiation pattern frequencies are slightly different from the theoretically calculated results, which is due to the fact that the physical parameters of the LWA have been optimized.

Fig. 4(d) presents the simulated normalized co-polarization and cross-polarization radiation patterns. It is obvious that the proposed LWA can achieve a full-space beam scanning from -90° to 90° within the relatively low cross-polarization. It should be noted that the gain in the upper hemisphere is slightly higher than the lower hemisphere, which is due to the fact that the patches and SSPPs feeding structure are not in the same plane, and the coupled energy is different in the two radiation directions.

III. EXPERIMENTAL VERIFICATION AND DISCUSSION

In order to experimentally verify the validity of the simulated results of the proposed LWA, as shown in Fig. 5(a), the designed

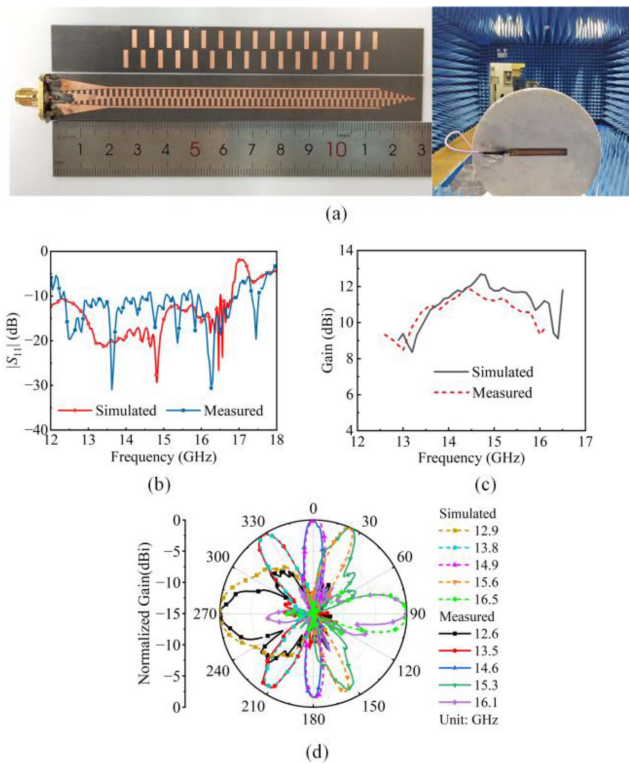


Fig. 5. (a) Structure of the proposed LWA fabricated prototype and measurement environment. Comparison of the simulated and measured results: (b) $|S_{11}|$ of the proposed LWA, (c) gain of the proposed LWA, and (d) normalized radiation patterns of the proposed LWA at different frequencies.

LWA is fabricated and measured in a far-field anechoic chamber. Fig. 5(b) and (c) present the comparison of the measured and simulated reflection coefficient and gain. It can be clearly seen that the proposed LWA can be operated well from 12.6 to 16.1 GHz and the range of gain from 8.5 to 12 dBi, which is generally consistent with the simulated results. Moreover, the measured normalized radiation pattern in the xoz -plane of the proposed LWA is drawn in Fig. 5(d), and the results indicate that the LWA achieves a 180° beam scanning from 12.6 to 16.1 GHz, the measured scanning rate is $7.38^\circ/\%$. Furthermore, from the comparison of the measured and simulated radiation pattern of the proposed LWA, it is obvious that there is a frequency shift in the measured results compared to the simulated ones, which may be due to manufacturing and measurement tolerances, as well as impedance mismatch from the SMA connector soldered.

To further demonstrate the advantages of the proposed LWA, the performance comparison of the proposed LWAs with the existing LWAs is given in Table I. The double-layer SSPP structure was used in [20]. Nevertheless, its performance was limited by the scanning angle and scanning rate. Reference [26] proposed a SIW-SSPP-based LWA, which achieved a high-scanning-rate performance. However, its scanning angle was not wide enough. Additionally, the various LWA structures were proposed in [28], [31], and [32] to achieve wide-angle beam scanning, and the full-space beam scanning LWA was proposed in [33] and [34]. Nevertheless, their scanning rate still needs to be improved. Compared to the above existing LWAs, our proposed LWA

TABLE I
PERFORMANCE COMPARISON OF LWA WITH OTHER
ANTENNAS OF THE SAME TYPE

Ref.	Antenna size ($\lambda_0 \times \lambda_0$)	Angle (deg)	Band width (GHz)	Scanning rate ($^\circ/\%$)	Avg. efficiency
[20]	8.5×1.65	134.3	9-24	1.48	80.7%
[26]	7.4×0.74	119	10.6-12.0	9.6	N/A
[28]	N/A	172	9.8-12.28	7.68	75.4%
[31]	7.9×1.3	155	5.5-20	1.36	83%
[32]	10.8×2.0	152	8.5-10.7	6.6	67%
[33]	9.2×0.9	180	6.3-9.1	4.95	87.4
[34]	8.84×1.19	180	22-29.8	5.98	78
This work	6.37×0.78	180	12.9-16.5	7.35	83.6%

* λ_0 is free space wavelength at center frequency.

*All data is simulated results.

has the advantages of a high-scanning rate, full-space beam scanning, and relatively compact size.

IV. CONCLUSION

In this letter, a full-space and high-scanning rate LWA based on SSPPs has been proposed, which mainly consists of SSPPs and the periodic metallic patch. EM waves are transmitted along the SSPP structure and are coupled to the metallic patches, which convert slow waves into fast waves and radiate energy into free space. Moreover, the dispersion relationship and space harmonics characteristics of the proposed design have been analyzed to explain the radiation mechanism. The proposed LWA realizes full-space beam scanning based on -1 order space harmonic and exhibits high-scanning rate by choosing the appropriate period of the patches. The measured results are generally consistent with the simulated ones, demonstrating that the proposed LWA can achieve full-space beam scanning from 12.6 to 16.1 GHz with a high-scanning rate of $7.35^\circ/\%$. The proposed LWA has a compact size, simple structure, wide scanning range, and high-scanning rate performance, which may be very useful in radar and satellite systems.

REFERENCES

- [1] R. Ranjan and J. Ghosh, "SIW-based leaky-wave antenna supporting wide range of beam scanning through broadside," *IEEE Antennas Wireless Propag. Lett.*, vol. 18, no. 4, pp. 606–610, Apr. 2019.
- [2] X. Zou, D. Yu, Y. Fan, J. Li, and W. Luo, "A substrate-integrated waveguide leaky-wave antenna based on eye-shaped transverse slot," *IEEE Trans. Antennas Propag.*, vol. 69, no. 11, pp. 7947–7952, Nov. 2021.
- [3] J. Liu and J. Liang, "Gain enhancement of transversely slotted substrate integrated waveguide leaky-wave antennas based on higher modes," *IEEE Trans. Antennas Propag.*, vol. 69, no. 8, pp. 4423–4438, Aug. 2021.
- [4] M. Wang, S. Sun, H. F. Ma, and T. J. Cui, "Supercompact and ultrawideband surface plasmonic bandpass filter," *IEEE Trans. Microw. Theory Techn.*, vol. 68, no. 2, pp. 732–740, Feb. 2020.
- [5] H. F. Ma, X. Shen, Q. Cheng, W. X. Jiang, and T. J. Cui, "Broadband and high-efficiency conversion from guided waves to spoof surface plasmon polaritons," *Laser Photon. Rev.*, vol. 8, no. 1, pp. 146–151, Jan. 2014.
- [6] L. Liu, Q. F. Fu, Y. J. Hu, G. Q. Luo, and L. Zhu, "An endfire controllable-filtering antenna based on spoof surface plasmon polaritons," *IEEE Antennas Wireless Propag. Lett.*, vol. 21, no. 3, pp. 526–530, Mar. 2022.
- [7] L. Zhao et al., "A novel broadband band-pass filter based on spoof surface plasmon polaritons," *Sci. Rep.*, vol. 6, no. 1, Dec. 2016, Art. no. 36069.

- [8] Y. Yi and A. Q. Zhang, "A tunable graphene filtering attenuator based on effective spoof surface plasmon polariton waveguide," *IEEE Trans. Microw. Theory Techn.*, vol. 68, no. 12, pp. 5169–5177, Dec. 2020.
- [9] Z. M. Chen et al., "A high efficiency band-pass filter based on CPW and quasi-spoof surface plasmon polaritons," *IEEE Access*, vol. 8, pp. 4311–4317, 2020.
- [10] J. Wang, L. Zhao, and Z.-C. Hao, "A band-pass filter based on the spoof surface plasmon polaritons and CPW-based coupling structure," *IEEE Access*, vol. 7, pp. 35089–35096, 2019.
- [11] S. Z. Yan et al., "A terahertz band-pass filter based on coplanar-waveguide and spoof surface plasmon polaritons," *IEEE Photon. Technol. Lett.*, vol. 34, no. 7, pp. 375–378, Apr. 2022.
- [12] B. C. Pan, P. Yu, Z. Liao, F. Zhu, and G. Q. Luo, "A compact filtering power divider based on spoof surface plasmon polaritons and substrate integrated waveguide," *IEEE Microw. Wireless Compon. Lett.*, vol. 32, no. 2, pp. 101–104, Feb. 2022.
- [13] T. Qiu, J. Wang, Y. Li, and S. Qu, "Circulator based on spoof surface plasmon polaritons," *IEEE Antennas Wireless Propag. Lett.*, vol. 16, pp. 821–824, 2017.
- [14] A. Kandwal, Q. F. Zhang, X. L. Tang, L. W. Liu, and G. Zhang, "Low-profile spoof surface plasmon polaritons traveling-wave antenna for near-endfire radiation," *IEEE Antennas Wireless Propag. Lett.*, vol. 17, no. 2, pp. 184–187, Feb. 2018.
- [15] X. B. Liu et al., "Frequency-scanning planar antenna based on spoof surface plasmon polariton," *IEEE Antennas Wireless Propag. Lett.*, vol. 16, pp. 165–168, 2017.
- [16] L. Yang, F. Xu, T. Jiang, J. Qiang, S. Liu, and J. Zhan, "A wideband high-gain endfire antenna based on spoof surface plasmon polaritons," *IEEE Antennas Wireless Propag. Lett.*, vol. 19, no. 12, pp. 2522–2525, Dec. 2020.
- [17] X. F. Zhang, J. Fan, and J. X. Chen, "High gain and high-efficiency millimeter-wave antenna based on spoof surface plasmon polaritons," *IEEE Trans. Antennas Propag.*, vol. 67, no. 1, pp. 687–691, Jan. 2019.
- [18] X. Lv, W. Cao, Z. Zeng, and S. Shi, "A circularly polarized frequency beam-scanning antenna fed by a microstrip spoof SPP transmission line," *IEEE Antennas Wireless Propag. Lett.*, vol. 17, no. 7, pp. 1329–1333, Jul. 2018.
- [19] Y. J. Han et al., "Multibeam antennas based on spoof surface plasmon polaritons mode coupling," *IEEE Trans. Antennas Propag.*, vol. 65, no. 3, pp. 1187–1192, Mar. 2017.
- [20] H. R. Zu, B. Wu, and T. Su, "Beam manipulation of antenna with large frequency-scanning angle based on field confinement of spoof surface plasmon polaritons," *IEEE Trans. Antennas Propag.*, vol. 70, no. 4, pp. 3022–3027, Apr. 2022.
- [21] J. Y. Yin et al., "Frequency-controlled broad-angle beam scanning of patch array fed by spoof surface plasmon polaritons," *IEEE Trans. Antennas Propag.*, vol. 64, no. 12, pp. 5181–5189, Dec. 2016.
- [22] Q. Zhang, Q. Zhang, and Y. Chen, "Spoof surface plasmon polariton leaky-wave antennas using periodically loaded patches above PEC and AMC ground planes," *IEEE Antennas Wireless Propag. Lett.*, vol. 16, pp. 3014–3017, 2017.
- [23] D. Liao, Y. Zhang, and H. Wang, "Wide-angle frequency-controlled beam-scanning antenna fed by standing wave based on the cutoff characteristics of spoof surface plasmon polaritons," *IEEE Antennas Wireless Propag. Lett.*, vol. 17, no. 7, pp. 1238–1241, Jul. 2018.
- [24] J. Wang, L. Zhao, Z.-C. Hao, and T. J. Cui, "Wide-angle frequency beam scanning antenna based on the higher-order modes of spoof surface plasmon polariton," *IEEE Trans. Antennas Propag.*, vol. 68, no. 11, pp. 7652–7657, Nov. 2020.
- [25] L. Ye, Z. Wang, J. Zhuo, F. Han, W. Li, and Q. H. Liu, "A back-fire to forward wide-angle beam steering leaky-wave antenna based on SSPPs," *IEEE Trans. Antennas Propag.*, vol. 70, no. 5, pp. 3237–3247, May 2022.
- [26] S. D. Xu et al., "A wide-angle narrowband leaky-wave antenna based on substrate integrated waveguide-spoof surface plasmon polariton structure," *IEEE Antennas Wireless Propag. Lett.*, vol. 18, no. 7, pp. 1386–1389, Jul. 2019.
- [27] M. Li, L. Zhu, D. Yi, and M. C. Tang, "A compact, high-efficiency, reflectionless leaky-wave antenna," *IEEE Antennas Wireless Propag. Lett.*, vol. 20, no. 6, pp. 888–892, Jun. 2021.
- [28] L. Jidi, X. Cao, J. Gao, T. Li, H. Yang, and S. Li, "Ultrawide-angle and high-scanning-rate leaky wave antenna based on spoof surface plasmon polaritons," *IEEE Trans. Antennas Propag.*, vol. 70, no. 3, pp. 2312–2317, Mar. 2022.
- [29] Y. Pan, Y. Cheng, and Y. Dong, "Surface plasmon polariton leaky-wave antennas with wideband arbitrary multibeam radiation," *IEEE Trans. Antennas Propag.*, vol. 70, no. 2, pp. 931–942, Feb. 2022.
- [30] X. Du, J. Ren, H. Li, C. Zhang, Y. Liu, and Y. Yin, "Design of a leaky-wave antenna featuring beam scanning from backfire utilizing odd-mode spoof surface plasmon polaritons," *IEEE Trans. Antennas Propag.*, vol. 69, no. 10, pp. 6971–6976, Oct. 2021.
- [31] K. Rudramuni et al., "Goubau-line leaky-wave antenna for wide-angle beam scanning from backfire to endfire," *IEEE Antennas Wireless Propag. Lett.*, vol. 17, no. 8, pp. 1571–1574, Aug. 2018.
- [32] G. Zhang, Q. Zhang, Y. Chen, and R. D. Murch, "High-scanning-rate and wide-angle leaky-wave antennas based on glide-symmetry Goubau line," *IEEE Trans. Antennas Propag.*, vol. 68, no. 4, pp. 2531–2540, Apr. 2020.
- [33] H. Jiang, X. Y. Cao, L. R. Jidi, H. H. Yang, and J. Gao, "A single-beam full-space scanning leaky-wave antenna with high-efficiency based on spoof surface plasmon polaritons," *Microw. Antennas Propag.*, vol. 16, no. 9, pp. 602–609, Jun. 2022.
- [34] D. Zhang, B. Wu, W.-H. Li, H.-R. Zu, X.-Z. Song, and T. Su, "Full-space-scanning substrate integrated waveguide antenna with enhanced scanning rate and efficiency," *IEEE Antennas Wireless Propag. Lett.*, vol. 22, no. 10, pp. 2517–2521, Oct. 2023.